Vol. 24 • No. 13 • April 2 • 2014

www.afm-journal.de

ADVANCED FUNCTIONAL MATERIALS

WILEY-VCH

Spinning Angora Rabbit Wool-Like Porous Fibers from a Non-Equilibrated Gelatin/Water/2-Propanol Mixture

*Philipp R. Stoessel, Robert N. Grass, Antoni Sánchez-Ferrer, Roland Fuhrer, Thomas Schweizer, Raffaele Mezzenga, and Wendelin J. Stark**

Due to their porous structure, angora rabbit fibers make for some of the highest quality wool. The application of these fibers on a technical scale is not feasible due to their limited availability and high price. Here, a robust fiber preparation method is reported based on an unusual spinning process, where a non-equilibrated, ternary system of protein, solvent, and non-solvent is continuously processed into strong fibers with minimal energy input and harmless solvents. Gelatin—the degradation product of collagen—is chosen as the protein component because of its immense availability from slaughterhouse waste. Due to the sponge-like structure of the ternary gelatin/water/2-propanol spinning mixture, fibers with internal cavities are produced. The porous nature of these fibers resembles the morphology of angora rabbit fibers. Despite their high porosity, the here-obtained gelatin fibers show clear re-orientation of the fibrous protein and attain a mechanical performance similar to other bio- (e.g., wool, tendon collagen) and synthetic polymers (e.g., polytetrafluoroethylene, polyamide 6). These promising results motivate for broader investigations on the spinning of non-equilibrium protein mixtures and suggest the use of porous gelatin fibers in textiles.

1. Introduction

Along with other specialty animal fibers such as cashmere, mohair or alpaca, angora rabbit fibers make up for some of the highest quality animal fibers of textile relevance.[1–3] Angora rabbit fibers stand out because of their shininess, small fiber diameter and the presence of a lattice-type medulla.[1,3,4] The latter is a hollow or partially filled central canal running lengthwise of the fibers, yielding a porous fiber structure and decreased fiber density.[3,5] In most animal fibers, medullated fibers are contaminants and have adverse effects on its value and end-use potential.[5,6] In contrast, angora rabbit fiber profits from the medulla structure in terms of superior insulation properties.[4] Despite their extraordinary properties, angora rabbit fibers are not suited for applications on a technical scale due to the limited natural availability (global production of about 10 000 tons per year) and high price (approximately 20 USD kg^{-1}).[7] There is a clear need for fibers which combine high porosity and good mechanical stability at the same time. Ideally, the fibers should be built up from biopolymers as there is permanent demand for environmentally friendly products.[8,9] A lot of biopolymers (e.g., polylactic acid) are synthetically produced from natural monomers and rely on starch sources such as corn or sugar cane.[9] Thus, they may compete with the food chain and endanger food security. To our understanding, it is beneficial to produce biopolymers from waste materials, e.g., proteins which are normally discarded. Proteins and peptides are extremely versatile building blocks for the fabrication of biomaterials.[10] A fibrous protein of high relevance is collagen, the most abundant structural protein in the extracellular matrix of multicellular animals and in vertebrates where it accounts for about 30–60 wt% of the total body protein.[11–13] Thus, collagen is a major component in animal slaughterhouse waste (including hides, bones, hoof, tendon, and horn) of which large proportions are discarded.[14–16] With more than 10 million tons of slaughterhouse waste per year in the European Union alone, animal by-products are an immense source of collagen.[17] If the water insoluble, quasi-crystalline collagen is partially denatured by partial thermal and chemical degradation, gelatin is prepared.[12,15,18] Conversion of collagen to water-soluble gelatin involves breaking covalent interchain and hydrogen bondings. The network of linked tropocollagen units is then transformed to a water-soluble system consisting of random chains with a much lower degree of internal order.[12,19,20] A recent study has put emphasis on the importance of applying materials science principles to understand biological materials. For collagen, the hierarchical structure consists of polypeptides, tropocollagen, fibrils and collagen fibers which allows predictions on the deformation behavior of collagen.[13] The sol–gel transition of gelatin involves protein chains to switch from the random coil conformation to the native, collagen-like triple helical structure.[12,21,22] If the triple helices are precisely aligned (e.g., by inducing stress), a renatured, collagen-like structure may be

P. R. Stoessel, Dr. R. N. Grass, Dr. R. Fuhrer, Prof. W. J. Stark
ETH Zurich, Department of Chemistry and Applied Biosciences
Institute for Chemical and Bioengineering
Wolfgang-Pauli-Strasse 10, CH-8093, Zurich, Switzerland
E-mail: wendelin.stark@chem.ethz.ch
Dr. T. Schweizer
ETH Zurich, Department of Materials
Institute of Polymers
Wolfgang-Pauli-Strasse 10, CH-8093, Zurich, Switzerland
Dr. A. Sánchez-Ferrer, Prof. R. Mezzenga
ETH Zurich, Department of Health Sciences and Technology
Food and Soft Materials
Schmelzbergstrasse 9, CH-8092, Zurich, Switzerland

DOI: 10.1002/adfm.201303321

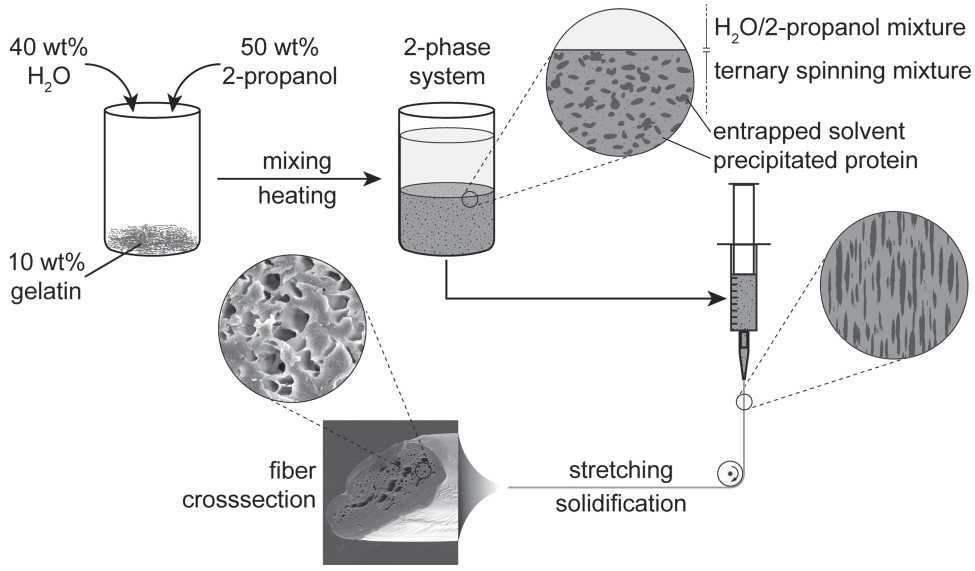

Figure 1. Dry spinning of a gelatin precipitate from a ternary mixture (gelatin/water/2-propanol) allows to continuously spin a porous protein fiber.

obtained.[12] It is expected that the induced anisotropy improves the mechanical performance of gelatin-based materials, which in their isotropic status is mechanically weak.[16,23]

In order to meet the introductory needs—fiber porosity and good mechanical properties as found in angora rabbit wool—a new fiber spinning process was developed. In a first step, a ternary mixture from gelatin, water and 2-propanol was prepared. This mixture is remarkable as it separates into two phases due to protein precipitation. The precipitate stands out because of its sponge-like structure and very good spinnability, which enabled simple spinning into a porous monofilament. **Figure 1** highlights the novelty of this process, namely the porous nature of the gelatin fibers as a results of the sponge-like structure of the protein precipitate. Gelatin or collagen fiber spinning has mostly been carried out by means of wet spinning,[11] gel spinning[24–26] or electrospinning;[27] these technological approaches produce dense protein fibers. In contrast, we opted for a dry spinning process, where the solidification of the polymer solution is achieved by solvent evaporation.[28] Owing to the high protein content and limited mobility of protein chains in the precipitate, one might argue that the presented process also has analogies to gel spinning. By continuously drawing the fiber in process, anisotropy was induced, which lead to improved mechanical properties.

In this study, we clearly demonstrate a reliable and continuous spinning process which allows producing porous biopolymer fibers in the kilometer scale. Despite their high porosity, the here obtained gelatin fibers attain mechanical performance similar to other bio- (e.g., wool, tendon collagen) and synthetic polymers (e.g., polytetrafluoroethylene, polyamide 6). Moreover, the fibers' degradability can be tuned by different crosslinking treatments. These promising results may pave the way to the large-scale production of artificial angora rabbit wool-like fibers.

2. Results and Discussion

2.1. Characterization of the Gelatin/Water/2-propanol Mixture

2.1.1. Appearance and Composition

Upon addition of 2-propanol (50 wt%) to deionized water (40 wt%) and gelatin powder (10 wt%) at 50 °C, the ternary system undergoes a phase separation (**Figure 2**a). This is in line

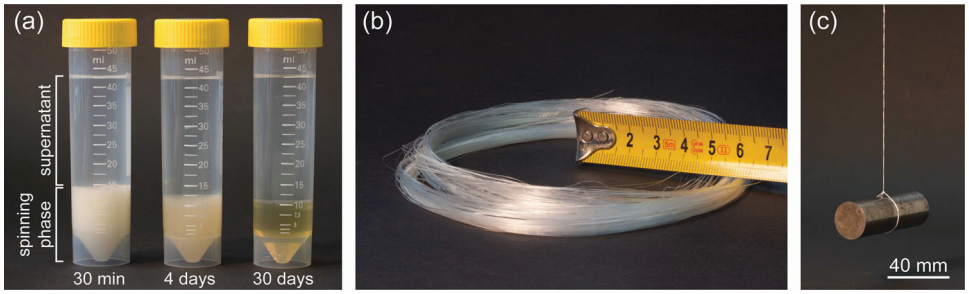

Figure 2. a) Two-phase, non-equilibrium gelatin/water/2-propanol mixture. 30 min after preparation, the opaque, lower phase (spinning phase) was fed to a spinning process, while the supernatant was discarded. Stability of the spinning raw material solution: after 30 days of storage at 50 °C the mixture became homogeneous (right; equilibration) and could no longer be spun. b) 300 meters of gelatin fiber spun at a stretching factor s = 1.6. c) Yarn of 10 monofilaments (s = 2) easily holding a weight of 140 g (17.8 MPa).

Table 1. Non-equilibrium, two-phase gelatin/water/2-propanol mixture; composition after different storage times. In the here presented spinning process, the spinning phase after 30 min was used.

	Sample after 30 min (3 min sedimentation)		Sample after 4 days		Sample after 30 days	
	Spinning phase	Supernatant	Spinning phase	Supernatant	Spinning phase	Supernatant
Gelatin [wt%]	27.0	0.1	36.0	0.0	36.1	0.0
Water [wt%]	41.2	46.8	39.3	37.3	41.5	27.9
2-propanol [wt%]	31.8	53.1	24.7	62.7	22.4	72.1

with previous reports on the addition of a water-miscible organic solvent to aqueous gelatin solutions leading to precipitation of the protein. This effect is often made use of in the context of nanoprecipitation for the production of polymeric nanoparticles.[28,29] In a study on poly(L-lactic acid) fibers, Qi et al. (2009) similarly characterized a ternary system of poly(L-lactic acid)/solvent/non-solvent, which underwent phase separation while being electrospun into nanofibers.[30] In the present work, a two-phase system with a lower gelatin-rich opaque phase (spinning phase) and an upper solvent-rich phase (supernatant) was obtained. Observing the gelatin/water/2-propanol mixture at 50 °C over a prolonged storage time without shaking indicated that the system is not in an equilibrium state (Figure 2a): after several days, the spinning phase compacted, became transparent (similar to an aqueous gelatin solution) and could no longer be spun. In order to reach the non-equilibrium state, the stored mixture could simply be shaken up and dry spinning of the opaque spinning phase was again possible. Gas chromatography (GC) and gravimetric analysis were used to determine the composition of the two-phase system at 50 °C over the storage time. The respective results are summarized in **Table 1**. From these numbers it follows that 2-propanol enriched in the supernatant over the storage time. Due to compacting of the spinning phase, gelatin and water percentage increased therein.

2.1.2. Rheology

Flow curves of the spinning phase and of an aqueous gelatin solution were recorded (see Supporting Information, Figure S1). The protein content was equal in both samples in order to permit comparison (27 wt% gelatin). The ternary spinning phase (gelatin/water/2-propanol) showed a higher zero-shear viscosity η_0 (9.1 Pa·s) than the reference gelatin solution (1.3 Pa·s). Additionally, a more prominent shear-thinning behavior was observed in the spinning phase. This is another indication that the organic solvent induced severe changes in the protein structure, which in turn resulted in exceptional spinnability and properties of the spinning phase. While destabilizing the native protein structure, organic solvents can stabilize secondary structures; it was e.g. found that denatured myoglobin at 70 % ethanol concentration possesses as many helical structures as the native protein.[31] This could explain the rheological behavior of our samples: while the aqueous gelatin solution was dominated by random peptide chains, the precipitated gelatin/water/2-propanol mixture contained structures of higher order, e.g., (triple-)helical structures and/or protein aggregates. This resulted in a higher η_0 and distinctive shear-thinning.

2.2. Characterization of Non-Crosslinked Gelatin Fibers

Gelatin fibers were obtained by extruding the spinning phase through a nozzle. Unspecific stretching was achieved by gravitational force and active stretching was achieved with the help of motorized rollers. The stretching factor s relates to the active fiber stretching and corresponds to the draw ratio on the roller system.

In Figure 2b, a long gelatin monofilament (stretching factor s = 1.6, diameter ~ 110 µm) is depicted. Figure 2c shows a manually fabricated yarn (10 filaments), holding a balance weight.

2.2.1. Mechanical Properties

Exemplary true stress vs. true strain curves for gelatin fibers produced at different stretching factors are indicated in **Figure 3**. Unstretched fibers (denoted by s = "0") were sampled directly after the spinning nozzle. All fibers showed a yield point followed by strain hardening. It is common for biopolymers to show an inflection point in the stress vs. strain curve.[13] In their measurements of *A. pernyi* silk fiber, Fu et al. (2011) also determined a distinct yield point and strain hardening.[32] After leaving the spinning nozzle, the gelatin fiber underwent a sol-gel transformation and the so-called renaturation process took place, leading to network formation of triple-helical, pseudo-cristalline structures or single protein chains.[12,21,22] The stretching of fibers can either be done during or after gelation. In the latter case, the fibers are e.g. swollen in a hydrophilic solvent to make them stretchable. In our spinning

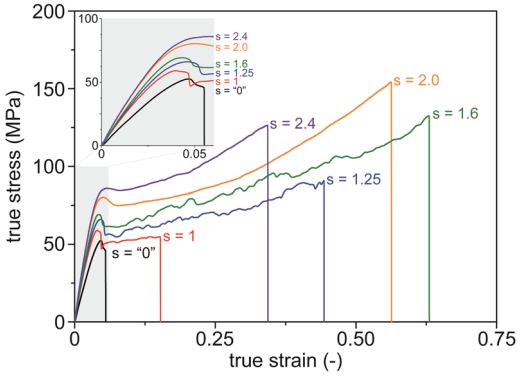

Figure 3. Illustrative true stress vs. true strain curves for selected gelatin fibers prepared at different stretching factors s (the ratio of different roller speeds, during active stretching). Reference fiber samples denoted with s = "0" were taken directly after the syringe. The inset displays an enlargement of the tensile test curves.

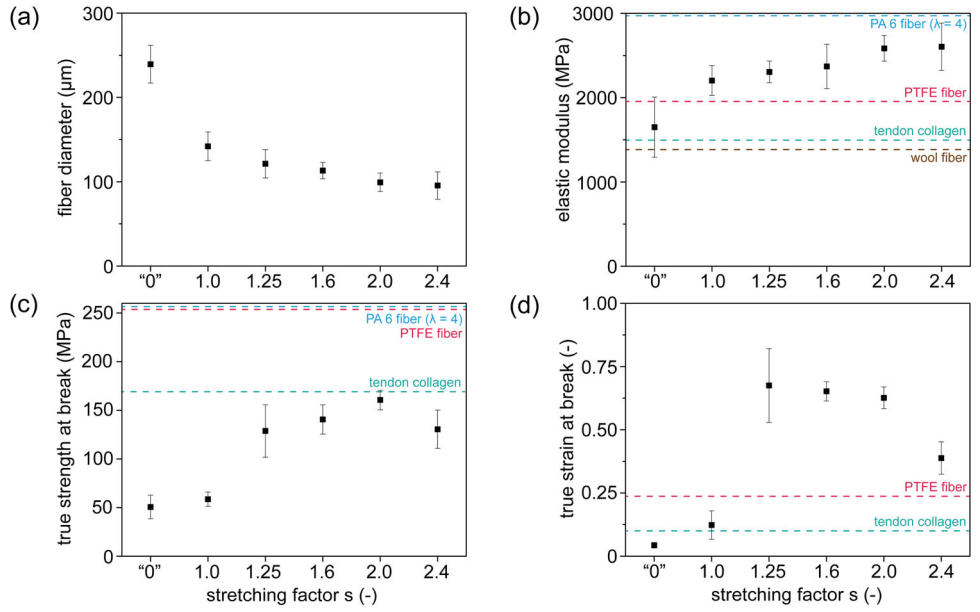

Figure 4. Apparent mechanical properties of non-crosslinked gelatin fibers spun at different stretching factors s (ratio of different roller speeds). The values are not corrected for fiber porosity. a) Fiber diameter (corresponding to a circular cross-section), b) elastic modulus, c) true strength at break and d) true strain at break. With increasing stretching, the fiber diameter decreased and the mechanical properties increased. Dotted lines indicate reference values for different polymer fibers produced and/or measured by other authors.[35,36]

process, the fibers are directly subjected to drawing (combination of unspecific and active stretching) in order to make the process attractive for a continuous large-scale production. Several reports have demonstrated that the mechanical properties of gelatin fibers or films can be improved by drawing because (1) segmental orientation of the fibrous protein is induced, (2) the development of triple-helical structures is facilitated and because (3) the overall material structure is improved (reduction in size and quantity of defects).[16,24,25,27,33,34] These findings could be confirmed in the present study as the mechanical properties were clearly enhanced by stretching the fibers. The average values of the apparent mechanical parameters are summarized in **Figure 4**; toughness values are given in the Supporting Information, Figure S2. As a consequence of mass conservation, the fiber diameter (corresponding to a circular cross-section) decreased from 240 ± 22 µm (s = "0") to 96 ± 16 µm (s = 2.4). By increasing the stretching factor, the elastic modulus increased from 1650 ± 356 MPa (s = "0") to 2604 ± 282 MPa (s = 2.4), the true tensile strength increased more than threefold from 51 ± 12 MPa (s = "0") to 161 ± 10 MPa (s = 2.0), the true strain at break from 0.04 ± 0.01 (s = "0") to 0.68 ± 0.15 (s = 1.25) and the toughness from 3 ± 5 MPa (s = "0") to 62 ± 6 MPa (s = 2.0). It must be noted that the above values have not been corrected for fiber porosity and that the effective mechanical properties would be significantly higher. While the elastic modulus reached a maximum at the highest stretching factor (s = 2.4), maximal strength, strain and toughness were obtained at slightly lower stretching. Compared to other stretching factors, the fibers with s = 2.4 frequently broke during the spinning process. It is assumed that they were overstrained, leading to structural defects, brittleness and lower strength. Altogether, drawing the fibers at s = 2 delivered the best results with simultaneous high modulus, strength, strain at break and toughness. This is of particular interest because most materials show a clear strength-toughness trade-off and only some biological composite materials have high strength and toughness at the same time.[34]

The above mechanical properties of gelatin fibers are on par with other biopolymers, biomaterials or some synthetic polymers.[35,36] Fukae and Midorikawa (2008) have reported a method for gel spinning non-porous gelatin fibers with the help of dimethyl sulfoxide, ethylene glycol or glycerol as solvent and methanol as coagulation agent, resulting in non-crosslinked fibers with elastic moduli of up to 3100 MPa and tensile strength of up to 157 MPa.[26] With an adapted method, Midorikawa et al. (2012) achieved even higher mechanical properties (up to 400 MPa tensile strength).[25] Compared to high-performance fibers such as fibers from carbon nanotubes (CNT)[37] or polymer composites filled with CNTs or carbon black,[38] the here presented gelatin fibers may appear weak. It must be noted, though, that high-performance fibers have drawbacks (e.g. brittleness, costs, environmental concerns) and for many applications, the gelatin fibers' properties are sufficient. Particularly, if targeting textile applications (e.g. artificial angora rabbit wool), the prepared fibers are similar to natural fibers or hair.[36,39]

2.2.2. Wide-Angle X-Ray Scattering (WAXS)

Referring to published reports,[18,19,40–42] the X-ray diffraction pattern of native collagen shows three prominent reflections: a strong inner equatorial spacing at $d_1 \approx 10$–16 Å ($2\theta \approx 8°$), a diffuse equatorial halo at $d_2 \approx 4.6$ Å ($2\theta \approx 20°$) and a strong meridional spacing at $d_3 \approx 2.9$ Å ($2\theta \approx 31°$). The spacing at $d_3 \approx 2.9$ Å represents the interplanar distance across the fiber axis, corresponding to the mean distance between amino acid residue sequence (Gly-X-Y repeats).[11,26,41] The spacing at $d_2 \approx 4.6$ Å

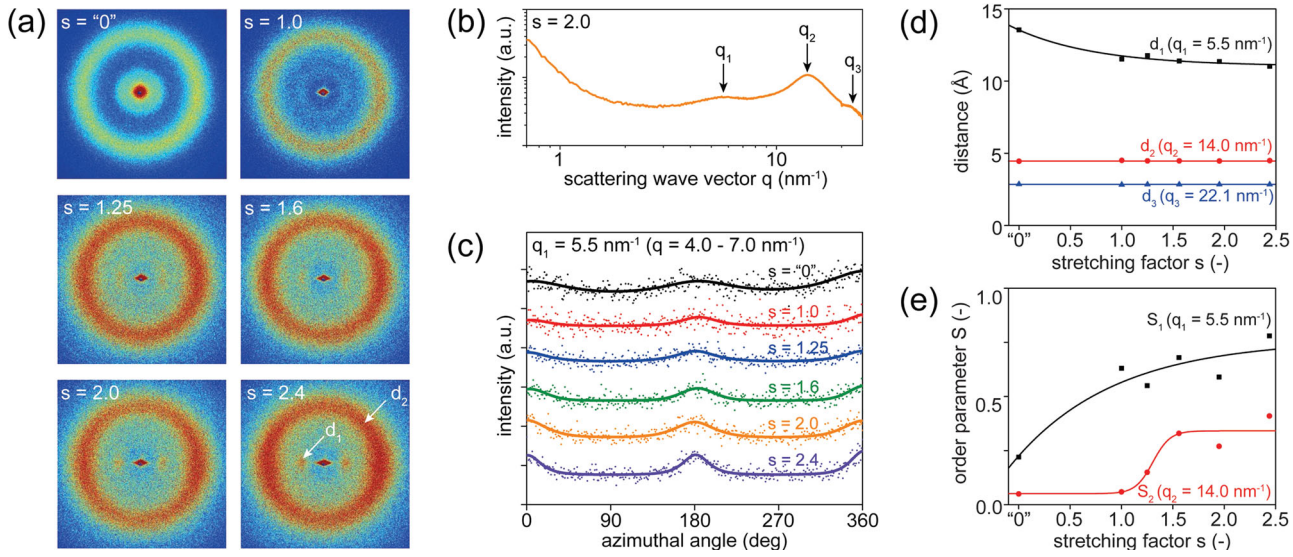

Figure 5. a) 2D wide-angle X-ray scattering (WAXS) of gelatin fibers prepared at different stretching factors s (ratio of different roller speeds). The unstretched gelatin fiber (s = "0") only shows diffuse rings for the reflections corresponding to the spacings d_1 = 11 Å and d_2 = 4.6 Å, indicating isotropic orientation at these length scales. For stretched fibers, the reflections at d_1 and d_2 get clearer and two-equatorial maxima start to appear. This demonstrates that the developed spinning process induces orientation in the fibrous protein. b) 1D wide-angle X-ray scattering intensity distribution for a gelatin fiber (s = 2). c) Azimuthal intensity distributions for scattering wave vector q_1 of gelatin fibers prepared at different stretching factors. d) Distances of the three prominent X-ray reflections of gelatin fibers prepared at different stretching factors. While distance d_1 decreases with stretching due to alignment of the gelatin's triple helices, d_2 and d_3 are constant over the spectrum of differently spun fibers. e) Order parameter S at the scattering wave vector q_1 (corresponding to the distance between triple helices, d_1 = 1.1 nm) and q_2 (distance between single helices, d_2 = 4.6 Å) of the gelatin fibers prepared at different stretching factors.

is practically the same for all proteins and corresponds to the mean distance between neighboring peptide chains (backbone spacing).[41] The reflection at $d_1 \approx 11$ Å is assigned to the intermolecular lateral packaging of the triple-helices.[40] The WAXS patterns of gelatin fibers are depicted in **Figure 5**a. The reflection at 2.9 Å is not visible on the scattering patterns by eye but can be observed in the 1D scattering intensity distribution (Figure 5b). The least stretched fibers (s = "0" and s = 1) showed an isotropic distribution pattern with a diffuse ring at d_2, indicating that the protein chains were randomly distributed. It is concluded that the unspecific stretching in the spinning tube has a minor effect on the fiber structure. Active stretching on motorized rollers (indicated by stretching factor s = 1.0–2.4) is more effective in inducing orientation: at stretching factors s ≥ 1.25, the two collagen-characteristic equatorial reflections at d_1 and two maxima at d_2 appeared. For scattering wave vector q_1, this is also illustrated by the azimuthal intensity distributions for different gelatin fiber samples (Figure 5c). This anisotropy indicates that the drawn gelatin fibers are partially renatured (coil-to-helix transition) and that the gelatin fibers comprise highly ordered domains. Parts of the protein chains recover their native conformation in the sol-gel transformation; other chains stay in the random coil conformation.[21] However, the single chains can also be oriented. A plot of the spacing distances vs. the stretching factor (Figure 5d) revealed, that the spacing distances d_2 and d_3 stayed constant, while d_1 was reduced with increasing fiber stretching from 13.5 to 11.0 Å due to alignment of the triple-helical structures. In order to quantify the anisotropy of the gelatin fibers, the order parameter S corresponding to the d_1 spacing (scattering wave vector q_1 = 5.5 nm^{-1}) and to the d_2 spacing (scattering wave vector q_2 = 14.0 nm^{-1}) was calculated. The results are summarized in Figure 5e. For both characteristic spacings, the order parameter increased with stretching of the fibers. Isotropic systems are characterized by S = 0, and uniaxially oriented crystalline systems have S = 1. For d_1 (distance between triple helices), S_{max} was 0.78 and for d_2 (distance between single peptide chains) S_{max} was 0.41. Accordingly, the gelatin fibers correspond to a highly oriented structure with (triple and single) helical domains aligned along the fiber axis.

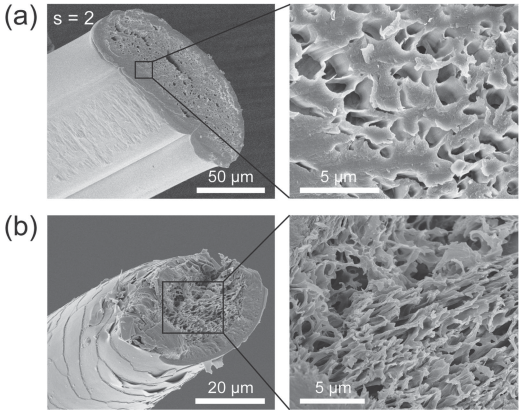

Figure 6. a) Scanning electron microscopy (SEM) images of a gelatin fiber cross-section (s = 2). The pore area was measured at different spots and the porosity was determined to be 30%. b) SEM micrographs of an angora rabbit fiber clearly show the morphological similarity to the here produced porous gelatin fibers.

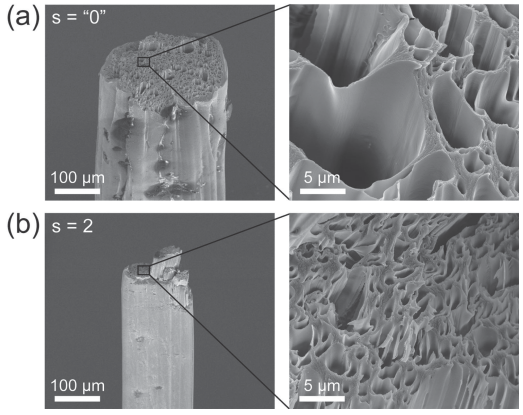

Figure 7. Scanning electron microscopy (SEM) images of fracture sites of gelatin fibers after tensile testing (strain rate 0.6 min^{-1}). a) The unoriented gelatin fibers (s = "0") show a straight fracture while the breaking of b) stretched fibers (s = 2) resulted in a fibrous fracture site.

2.2.3. Scanning Electron Microscopy (SEM)

SEM micrographs of a gelatin fiber exhibited elliptical cross-sections and a furrow in the longitudinal direction which is attributed to the nozzle design and the flattening on the rollers (see **Figure 6**a). This morphology is in good agreement with other results.[25] Furthermore, the fibers exhibited high porosity (~30%) due to solvent droplets which were enclosed in the spinning phase and evaporated in the spinning process. The average pore size of a gelatin fiber (s = 2) was ~1 µm. This immediately highlights that the bulk apparent mechanical properties evaluated above, would need to be rescaled by effective volume fractions, pointing at higher values. Featuring good mechanical properties and high porosity at the same time is highly interesting. To allow comparison of the gelatin fibers to angora rabbit fibers SEM micrographs of the animal fibers were taken (Figure 6b). The presence of the lattice-type medulla, which causes the porous fiber structure, was verified and the similarity to the porous gelatin fibers is evident. As in most animal keratin fibers, the angora rabbit fibers' surface is characterized by overlapping cuticle cells, whereas the artifical gelatin fibers have a smooth surface. The SEM micrographs in **Figure 7** show fracture sites of gelatin fibers which were subjected to a tensile test. The breaking site of an unoriented fiber (s = "0") was straight and sharp (Figure 7a), while for an oriented fiber (s = 2) it was fringy and fibrous (Figure 7b). This result again confirms that anisotropy was introduced by stretching the fiber in the spinning process.

2.3. Crosslinking Treatment and Swelling Experiments

Gelatin, as virtually all biopolymers, is water soluble and its properties are highly dependent on the water in the structure.[13,43] While being advantageous in degradation, the moisture sensitivity limits the application of gelatin products.[43,44] For this reason protein structures are often crosslinked to reduce the swelling behavior and the rate of biodegradation. In this study, formaldehyde in the gas phase, FA(g), was used for chemically crosslinking the gelatin fibers (s = 2) during 1 or 15 h. FA was chosen for its small molecular size (good diffusion), low cost (only a fraction of other crosslinkers) and widespread use in the tanning and pharmaceutical industry.[45,46] Crosslinking in the gas phase is advantageous over solution-based crosslinking because the anisotropic protein structure is not affected by solvents/swelling. Formaldehyde-treated protein fibers were also physically crosslinked by dehydrothermal treatment (DHT). DHT involves both the removal of residual moisture and the formation of covalent peptide bonds, especially ester and amide bonds.[47]

The appearance and the obtained mechanical properties of (crosslinked) gelatin fibers, which were subjected to swelling in deionized water for 24 hours, are illustrated in **Figure 8**. The non-crosslinked fibers swelled in a matter of seconds, lost shape and became transparent. The swelling of crosslinked fibers (1 h FA(g)) was less pronounced and slower, while the crosslinked fibers (15 h FA(g)) did only minimally swell. As revealed by Figure 8a, the non-crosslinked fibers and the 1 h crosslinked fibers evidentially sunk in the water because of water up-take. The 15 h crosslinked fibers still floated, indicating that the low density of the porous fiber was maintained and that water was not incorporated into the fiber matrix. The reduction of swelling was additionally monitored by fiber diameter measurements (Figure 8b): a fourfold reduction in swelling was observed in well crosslinked fibers (15 h FA(g) & DHT). These findings are in accordance with Fakirov et al. (1996), who stated that crosslinked gelatin is insoluble in water but it is still swollen by it.[16] Drying the swollen samples caused the fibers to shrink, resulting in equal cross-sectional areas as before swelling. The elastic moduli are indicated in Figure 8c. When being tested in the wet state, fibers which were not crosslinked or only treated by FA did not show an elastic regime (see inset with schematic stress vs. strain curve in Figure 8c). However, combining FA crosslinking and DHT had a distinct effect on wet state stiffness and yielded an elastic modulus of 430 MPa. As shown by Bhushan (2010), human hair also swells in water and the elastic modulus follows a similar pattern as observed in this study: soaking hair in water decreases the elastic modulus from about 3000 MPa to 500–900 MPa, while subsequent drying reestablishes the original elastic modulus.[39] It is known that formaldehyde exhibits a fast diffusion rate, while having very slow endpoint fixation rates.[48] Working with fish gelatin films and formaldehyde, Fraga and Williams (1985) concluded that the crosslinking reaction has a threshold temperature at 100 °C.[20] Galembeck et al. (1977) concluded that crosslinking proteins with formaldehyde at room temperature and neutrality is slow.[46] This would explain why crosslinking with gaseous formaldehyde at room temperature took several hours, while still not yielding satisfying wet state behavior of the fibers. Obviously, the DHT treatment did also have a positive side effect in increasing the reaction rate of FA. The true strength at break (Figure 8d) strongly decreased due to swelling: for non-crosslinked fibers it was as low as 0.3 MPa, while 15 h FA(g) or 15 h FA(g) & DHT resulted in about 20 MPa strength. Compared to the initial results before swelling, the mechanical properties after swelling and drying increased to a small extent. Presumably, the swelling helped to diminish internal tension and defects in the fibers or the handling of gelatin fibers in swollen state led to further stretching of the fibrous structure.

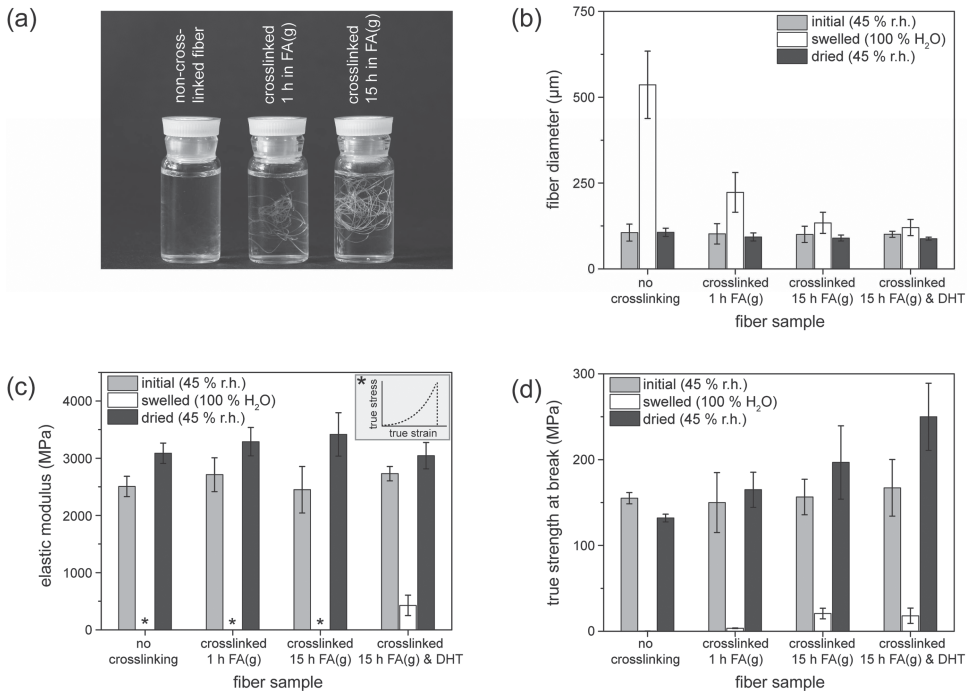

Figure 8. Appearance and mechanical properties of gelatin fibers (s = 2) as a function of crosslinking and swelling. a) Fiber integrity after 24 h of swelling in deionized water after crosslinking. Non-crosslinked fibers swell in a matter of minutes and become transparent. Fibers crosslinked for 1 h swell to a lesser degree while crosslinking for 15 h strongly increases the water resistance. b) Fiber diameter (corresponding to a circular cross-section), c) elastic modulus (*: no elastic regime in the stress vs. strain curve), and d) true tensile strength of gelatin fibers before swelling, in swelled state (24 h in deionized water) and after swelling with subsequent drying. By combining formaldehyde crosslinking with a dehydrothermal treatment, the stiffness (elastic modulus) of the swelled fibers could clearly be increased.

3. Conclusion

The prominent advantages of gelatin are biodegradability, versatility and an immense availability from slaughterhouse waste. Because of its poor mechanical properties, untreated gelatin is hardly able to substitute synthetic polymers. However, it is generally acknowledged that the physical properties can be improved by promoting the renaturation of collagen, i.e. the aligning of triple helical structures. In this work, a spinning process for the fabrication of gelatin fibers is proposed, which only requires harmless solvents and minimal energy input. **Table 2** summarizes the major characteristics of the new process and relates it to the established methods for gelatin fiber spinning found in the literature. Unlike the other methods, the here presented process is special owing to the fact that porous fibers are produced. Furthermore, it simultaneously allows continuous spinning and drawing of the gelatin fibers. XRD measurements showed that the suggested orientation of single helices and triple helices was indeed achieved. Tensile tests revealed that stretching the fibers during the spinning improves the mechanical properties to the point where gelatin fibers can compete with other biopolymers and synthetic polymers. This is even more promising as the fibers are characterized by high porosity (up to 30%), as observed by SEM. In a further treatment step, the fibers were crosslinked by gaseous formaldehyde and dehydrothermal treatment. This crosslinking combination significantly increased the water resistance of the gelatin fibers to nearly the level of human hair.

Table 2. Overview of different spinning processes for gelatin/collagen fiber production.

Source	Process	Principle	Product
this work	dry spinning	spinning of non-equilibrium gelatin/water/2-propanol mixture; simultaneous stretching and solidification	porous fibers
Midorikawa et al. (2012)[25]	gel spinning	spinning gelatin/ethylene glyocol gel; coagulation in cold methanol; extraction of ethylene glycol in methanol (10 days); drying	dense fibers
Fukae and Midorikawa (2008)[26]	gel spinning	spinning gelatin/DMSO gel; coagulation in cold methanol; batch-wise drawing of fibers; extraction of DMSO in methanol (10 days); drying	dense fibers
Meyer et al. (2010)[11]	wet spinning	spinning of collagen dispersion; coagulation in ethanol/acetone; drying	dense fibers
Ayres et al. (2007)[27]	electrospinning	gelatin in trifluoroethanol spun at 25 kV accelerating voltage	smooth scaffolds

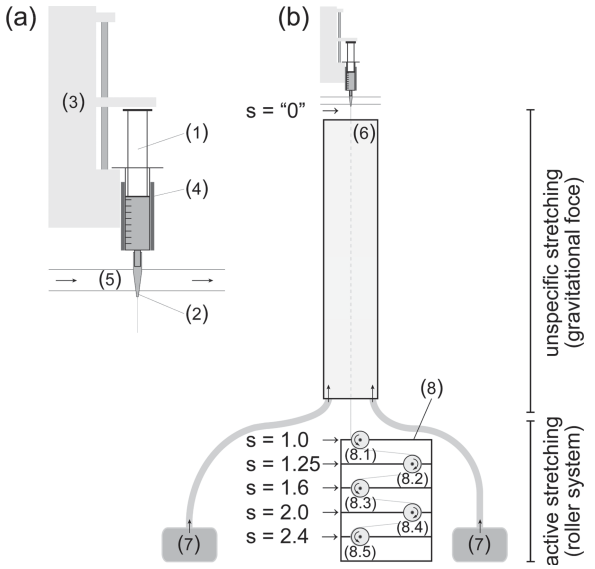

Figure 9. a) Detailed view of the syringe pump and b) overview of the spinning machinery for gelatin fiber production. It consists of (1) plastic syringe (25 mL), (2) plastic syringe nozzle (0.8 mm opening diameter), (3) syringe pump run at Q = 0.2 mL min^{-1}, (4) heating pad for syringe at 45 °C, (5) circulating water bath at 35 °C for syringe nozzle heating, (6) spinning tube of 2.5 m length and 0.25 m diameter, (7) humidifiers to ensure constant humidity (50 ± 5 % relative humidity) and (8) motorized stretching device with rollers (8.1–8.5) running at 16 to 40 rpm in order to work at different stretching factors s.

The resemblance of the produced gelatin fibers with highest quality natural fibers—such as angora rabbit fibers—is remarkable. These advantageous properties suggest the use of porous gelatin fibers in different forms (single fiber, yarn or woven structure) in textile applications.

4. Experimental Section

Preparation of Gelatin/Water/2-Propanol Mixture and Spinning Process: Type A gelatin from porcine skin (G2500, ~300 g Bloom strength) and 2-propanol (HPLC-grade) were used as received from Sigma-Aldrich. Deionized water (40 wt%) and 2-propanol (50 wt%) were added to gelatin powder (10 wt%). The mixture was tempered in a water bath at 50 °C for 30 min and shaken by hand every 5 min. This yielded a 2-phase system with an opaque, gelatin-rich lower phase (spinning phase) and an upper solvent-rich phase (supernatant). Subsequent to sedimentation (3 min), the supernatant was decanted and the lower gelatin-rich phase was transferred to a plastic syringe (25 mL), tempered at 45 °C. As illustrated in **Figure 9**, the spinning phase was extruded as a monofilament through a tempered syringe nozzle (35 °C) into a vertical spinning tube (50 ± 5 % relative humidity, 23 ± 2 °C) where evaporation and unspecific stretching by gravitational force took place. Active fiber stretching and evaporation of residual solvent was achieved by transferring the fiber onto a motorized stretching device with motorized rollers. The speed of roller 1 was adjusted to match the speed of the falling fiber (~16 rpm). The successive rollers were each accelerated by a factor of 1.25. The ratio of different roller speeds was defined as stretching factor s, ranging from s = 1.25 (roller 2), s = 1.56 (roller 3), s = 1.95 (roller 4) to s = 2.4 (roller 5). Depending on the chosen roller for fiber uptake, gelatin fibers at different stretching factors were prepared. For the purpose of reference, fiber samples were also taken directly after the syringe nozzle and denoted with s = "0".

Crosslinking Treatment and Swelling Experiments: Gas-phase crosslinking of gelatin fibers (s = 2) was achieved by exposing them to formaldehyde (10 mL, Sigma-Aldrich, > 34.5 wt%) in a desiccator. The treatment was conducted for either 1 or 15 h at room temperature (23 ± 2 °C). An aliquot of FA crosslinked fibers (15 h) was further subjected to dehydrothermal treatment (DHT). The fibers were placed in a vacuum oven (120 °C, 50 mbar) for 10 h. After crosslinking, the fibers were equilibrated at room temperature and 45 ± 5% relative humidity. Fibers with no, 1 h FA(g), 15 h FA(g) and 15 h FA(g)&DHT treatment were swelled in deionized water for 24 h. The mechanical properties (elastic modulus, true tensile strength) were measured before, directly after swelling (wet state) and after swelling with subsequent drying at 45 ± 5% relative humidity (dry state).

Characterization of Gelatin/Water/2-Propanol Mixture: The gelatin/water/2-propanol mixture was kept in a water bath at 50 °C and sampled after different storage times of 30 min, 4 days, and 30 days. The supernatant was centrifuged (15 000 g, 20 s) and a precise amount of 1-octanol (Fluka, puriss.) was added as internal standard. The spinning phase was transferred into a round bottom flask and distilled into a second flask containing a defined amount of 1-octanol as internal standard. The solvent samples were analyzed using a Hewlett Packard 6890 Series gas chromatograph equipped with a phenyl methyl siloxane column (HP-5MS) and a flame ionization detector (GC-FID). Helium was used as carrier gas (1 mL min^{-1}) and the oven temperature was increased from 50 to 250 °C at a rate of 20 °C min^{-1}. An appropriate GC-FID response factor was determined to quantify 2-propanol and 1-octanol. The dry weight of gelatin was gravimetrically determined. Water content was calculated as the residual weight percentage.

Rheological measurements were performed on a Paar Physica MCR300 rheometer equipped with a cone-plate geometry (diameter 30 mm, cone-angle 4°) and a Peltier element (set at 50 °C). The lower phase of a fresh gelatin/water/2-propanol mixture (spinning phase) and a 27 wt% aqueous gelatin solution (reference) were sheared from 0.1 to 22 s^{-1} and the flow curves recorded.

Fiber Characterization: Gelatin fibers were stored at room temperature (23 ± 2 °C) and constant humidity (45 ± 5% relative humidity) for 2 days. Tensile tests (n = 6) were conducted according to ASTM D3822–07 on a Shimadzu Universal Testing Instrument AGS-X equipped with a 100 N load cell and pneumatic clamps. Fiber specimens (40 ± 1 mm) were tested at constant speed (24 mm min^{-1}). The cross-sectional area of every specimen was optically measured by light microscopy (Zeiss Axio Imager.M2m) and the appropriate dimension, representing the diameter of a corresponding circle, was calculated. In selected fiber samples, the cross-sectional area was cross checked by scanning electron microscopy (SEM, FEI, NovaNanoSEM 450) and imaging software (ImageJ, version 1.46). The porosity was not accounted for, though. Instead, the bulk apparent mechanical properties (elastic modulus (between 0.001 and 0.005 strain), true tensile strength, true strain at break, toughness (= area under the curve)) were determined from the stress vs. strain curves.

Wide-angle X-ray scattering (WAXS) experiments were performed using a Rigaku MicroMax-002+ microfocused beam (4 kW, 45 kV, 0.88 mA). The Cu Kα radiation ($\lambda_{Cu\ K\alpha}$ = 1.5418 Å) was collimated by three pinhole collimators and a bundle of parallel-aligned fibers was vertically placed to the detector. The scattered X-ray intensity was detected by a Fuji Film BAS-MS 2025 imaging plate system. An effective scattering-vector range of 0.5 nm^{-1} < q < 25 nm^{-1} was obtained, where q is the scattering wave vector defined as $q = 4\pi \sin\theta/\lambda_{Cu\ K\alpha}$, with a scattering angle of 2θ. From the scattering intensities, the order parameter S was calculated. The order parameter S was determined according to Lovell and Mitchell and is given in the Supporting Information (Equation (1)).[49]

The fiber's morphology was investigated by means of scanning electron microscopy (FEI Nova NanoSEM 450, 5 kV). The samples were sputter-coated with a 3–4 nm platinum layer (Leica EM SCD005). Cross-sections of gelatin fibers were obtained by freezing a fiber sample in liquid nitrogen for 30 s followed by cutting with a scalpel. Imaging software (ImageJ, version 1.46) was used to determine the cross-

sectional area, the average pore diameter and the pore area for porosity calculation. The porosity was calculated by dividing the pore area by the total cross-sectional area.

Supporting Information

Supporting Information is available from the Wiley Online Library or from the author.

Acknowledgements

We are grateful to Urs Krebs and Max Wohlwend for spinning machinery construction. We thank Daniela Paunescu and Robert Niffeler for providing the angora rabbit fiber samples. Financial support by ETH Zurich is kindly acknowledged.

Received: September 26, 2013
Published online: November 27, 2013

[1] a) L. Onal, M. Korkmaz, M. Tutak, *Fiber. Polym.* **2007**, *8*, 198; b) K. D. Langley, T. A. Kennedy, *Text. Res. J.* **1981**, *51*, 703.
[2] S. A. Rafat, H. de Rochambeau, R. G. Thebault, I. David, S. Deretz, M. Bonnet, B. Pena-Arnaud, D. Allain, *Livest. Sci.* **2008**, *113*, 8.
[3] F. J. Wortmann, G. Wortmann, W. Arns, *Text. Res. J.* **1989**, *59*, 73.
[4] N. Oglakcioglu, P. Celik, T. B. Ute, A. Marmarali, H. Kadoglu, *Text. Res. J.* **2009**, *79*, 888.
[5] B. A. McGregor, K. L. Butler, M. B. Ferguson, *Small Ruminant Res.* **2013**, *113*, 90.
[6] C. J. Lupton, F. A. Pfeiffer, N. E. Blakeman, *Small Ruminant Res.* **1991**, *5*, 357.
[7] A. C. Schlink, S. M. Liu, *Angora Rabbits – A Potential New Industry for Australia*, Rural Industries Research and Development Corporation, Kingston **2003**.
[8] A. A. Apostolov, D. Boneva, E. Vassileva, J. E. Mark, S. Fakirov, *J. Appl. Polym. Sci.* **2000**, *76*, 2041.
[9] A. K. Mohanty, M. Misra, G. Hinrichsen, *Macromol. Mater. Eng.* **2000**, *276/277*, 1.
[10] S. G. Zhang, *Nat. Biotechnol.* **2003**, *21*, 1171.
[11] M. Meyer, H. Baltzer, K. Schwikal, *Mater. Sci. Eng., C* **2010**, *30*, 1266.
[12] A. Veis, *The Macromolecular Chemistry of Gelatin*, Academic Press, London **1964**.
[13] M. A. Meyers, J. McKittrick, P.-Y. Chen, *Science* **2013**, *339*, 773.
[14] a) M. M. Brooks, in Handbook of Textile Fibre Structure, Volume 2 (Eds: S. J. Eichhorn, J. W. S. Hearle, M. Jaffe, T. Kikutani), Woodhead Publishing, Cambridge **2009**, p. 234; b) B. Kherrati, M. Faid, M. Elyachioui, A. Wahmane, *Bioresour. Technol.* **1998**, *63*, 75.
[15] J. E. Eastoe, A. A. Leach, in *The Science and Technology of Gelatin* (Eds: A. G. Ward, A. Courts), Academic Press, London **1977**, p. 73.
[16] S. Fakirov, Z. Sarac, T. Anbar, B. Boz, I. Bahar, M. Evstatiev, A. A. Apostolov, J. E. Mark, A. Kloczkowski, *Colloid Polym. Sci.* **1996**, *274*, 334.
[17] B. Gminder, J. Reyniers, *Questions and Answers on Animal By-Products*, MEMO/04/107, European Commission, Brussels **2004**.
[18] W. F. Harrington, P. H. Von Hippel, *Adv. Protein Chem.* **1961**, *16*, 1.
[19] I. Pezron, M. Djabourov, L. Bosio, J. Leblond, *J. Polym. Sci. Part B Polym. Phys.* **1990**, *28*, 1823.
[20] A. N. Fraga, R. J. J. Williams, *Polymer* **1985**, *26*, 113.
[21] C. Joly-Duhamel, D. Hellio, M. Djabourov, *Langmuir* **2002**, *18*, 7208.
[22] a) M. Djabourov, J. Leblond, P. Papon, *J. Phys.* **1988**, *49*, 319; b) M. Gioffre, P. Torricelli, S. Panzavolta, K. Rubini, A. Bigi, *J. Bioact. Compat. Pol.* **2012**, *27*, 67.
[23] H. Chambi, C. Grosso, *Food Res. Int.* **2006**, *39*, 458.
[24] R. Fukae, A. Maekawa, S. Sangen, *Polymer* **2005**, *46*, 11193.
[25] T. Midorikawa, O. S. Lawal, Y. Sasaki, R. Fukae, *J. Appl. Polym. Sci.* **2012**, 1.
[26] R. Fukae, T. Midorikawa, *J. Appl. Polym. Sci.* **2008**, *110*, 4011.
[27] C. E. Ayres, G. L. Bowlin, R. Pizinger, L. T. Taylor, C. A. Keen, D. G. Simpson, *Acta Biomater.* **2007**, *3*, 651.
[28] T. Tsurumi, in *Advanced Fiber Spinning Technology* (Eds: T. Nakajima, K. Kajiwara, J. E. McIntyre), Woodhead Publishing Ldt, Cambridge **1994**, p. 65.
[29] a) K. Ofokansi, G. Winter, G. Fricker, C. Coester, *Eur. J. Pharm. Biopharm.* **2010**, *76*, 1; b) K. Kamide, S. Manabe, *ACS Sym. Ser.* **1985**, *269*, 197.
[30] Z. Qi, H. Yu, Y. Chen, M. Zhu, *Mater. Lett.* **2009**, *63*, 415.
[31] a) G. Conio, E. Patrone, S. Brighetti, *J. Biol. Chem.* **1970**, *245*, 3335; b) J. Hermans, D. Puett, G. Acampora, *Biochemistry* **1969**, *8*, 22.
[32] C. J. Fu, D. Porter, X. Chen, F. Vollrath, Z. Z. Shao, *Adv. Funct. Mater.* **2011**, *21*, 729.
[33] A. Bigi, B. Bracci, G. Cojazzi, S. Panzavolta, N. Roveri, *Biomaterials* **1998**, *19*, 2335; A. Tanioka, K. Miyasaka, K. Ishikawa, *Biopolymers* **1976**, *15*, 1505.
[34] D. Papkov, Y. Zou, M. N. Andalib, A. Goponenko, S. Z. D. Cheng, Y. A. Dzenis, *ACS Nano* **2013**, *7*, 3324.
[35] a) J. W. Cho, G. W. Lee, B. C. Chun, *J. Appl. Polym. Sci.* **1996**, *62*, 771; b) M. Goessi, T. Tervoort, P. Smith, *J. Mater. Sci.* **2007**, *42*, 7983; c) J. M. Gosline, P. A. Guerette, C. S. Ortlepp, K. N. Savage, *J. Exp. Biol.* **1999**, *202*, 3295.
[36] M. Feughelm, M. S. Robinson, *Text. Res. J.* **1971**, *41*, 469.
[37] N. Behabtu, C. C. Young, D. E. Tsentalovich, O. Kleinerman, X. Wang, A. W. K. Ma, E. A. Bengio, R. F. ter Waarbeek, J. J. de Jong, R. E. Hoogerwerf, S. B. Fairchild, J. B. Ferguson, B. Maruyama, J. Kono, Y. Talmon, Y. Cohen, M. J. Otto, M. Pasquali, *Science* **2013**, *339*, 182.
[38] H. Deng, T. Skipa, E. Bilotti, R. Zhang, D. Lellinger, L. Mezzo, Q. Fu, I. Alig, T. Peijs, *Adv. Funct. Mater.* **2010**, *20*, 1424.
[39] B. Bhushan, in *Biophysics of Human Hair*, Springer, Berlin Heidelberg **2010**, 57.
[40] G. Balian, J. H. Bowes, in *The Science and Technology of Gelatin* (Eds: A. G. Ward, A. Courts), Academic Press, London **1977**, p. 1.
[41] G. D. McLaughlin, E. R. Theis, *The Chemistry of Leather Manufacture* Reinhold Publishing Corporation, New York **1945**.
[42] K. H. Gustavson, *The Chemistry and Reactivity of Collagen* Academic Press Inc., New York **1956**.
[43] L. Yu, K. Dean, L. Li, *Prog. Polym. Sci.* **2006**, *31*, 576.
[44] I. Rault, V. Frei, D. Herbage, N. Abdul-Malak, A. Huc, *J. Mater. Sci.: Mater. Med.* **1996**, *7*, 215.
[45] C. Klockenbusch, J. Kast, *J. Biomed. Biotechnol.* **2010**, *2010*, 927585.
[46] F. Galembeck, D. S. Ryan, J. R. Whitaker, R. E. Feeney, *J. Agric. Food Chem.* **1977**, *25*, 238.
[47] a) M. C. Wang, G. D. Pins, F. H. Silver, *Biomaterials* **1994**, *15*, 507; b) C. M. Vaz, L. A. De Graaf, R. L. Reis, A. M. Cunha, *J. Mater. Sci.-Mater. Med.* **2003**, *14*, 789; c) I. V. Yannas, A. V. Tobolsky, *Nature* **1967**, *215*, 509; d) M. Madaghiele, A. Piccinno, M. Saponaro, A. Maffezzoli, A. Sannino, *J. Mater. Sci.-Mater. Med.* **2009**, *20*, 1979.
[48] J. H. Bedino, *An Official Publication of the Research and Education Department* The Champion Company, Springfield **2003**, *649*, p. 2614.
[49] a) R. Lovell, G. R. Mitchell, *Acta Crystallogr. A* **1981**, *37*, 135; b) G. R. Mitchell, A. H. Windle, in *Developments in Crystalline Polymers-2*, (Ed: D. C. Bassett), Elsevier Applied Science, London **1988**, p. 115.